IEEE Access
Multidisciplinary | Rapid Review | Open Access Journal

Received 13 January 2025, accepted 28 March 2025, date of publication 2 April 2025, date of current version 10 April 2025.

Digital Object Identifier 10.1109/ACCESS.2025.3557331

RESEARCH ARTICLE

Ship Magnetic Signature Classification Using GRU-Based Recurrent Neural Networks

KAJETAN ZIELONACKI, JAROSŁAW TARNAWSKI, AND MIROSLAW WOLOSZYN
Faculty of Electrical and Control Engineering, Gdańsk University of Technology, 80-233 Gdańsk, Poland

Corresponding author: Jarosław Tarnawski (jartarna@pg.edu.pl)

This work was supported in part by Gdańsk University of Technology through the Radium–Excellence Initiative–Research University Program under Grant 12/1/2023/IDUB/III.1a/Ra, and in part by the Technetium Talent Management under Grant 39/1/2024/IDUB/III.4c/Tc.

ABSTRACT Magnetic signatures represent the magnetic field generated by a ship's ferromagnetic components and provide valuable information for identifying vessels not only in naval operations, but also in civil passages. The topic of accurate modelling of these signatures is relevant to this day, but also the complexity of the model necessary to accurately predict the ship's magnetic field. This paper presents the implementation of a deep, recurrent neural network (RNN) designed for classification of compliance between the original magnetic signature of a ship and the one obtained from a model. Therefore, the quality of the model can be analyzed using a classifier during the modeling process. The necessity to introduce a tool for signature compliance classification arose during numerical modeling of a ship in Finite Element Method (FEM) environment as well as during reverse modeling based on data coming from measurements. Another application is the use of a shallow RNN for classifying ships by their size and type. A sufficient amount of data is rarely available and therefore data augmentation solution is necessary. The process of obtaining a large dataset of signals from a multi-dipole model and using an interpolation technique for generating training, validation and test data is comprehensively described. Methods used for selecting the best network structure and hyperparameter tuning using grid search and random search in order to achieve a satisfactory classification accuracy are thoroughly explained. Features, advantages and limitations of developed algorithms are derived strictly from the nature of neural networks.

INDEX TERMS Deep learning, gated recurrent unit, magnetic signature, signal processing.

I. INTRODUCTION

Magnetic signatures arise as a local disturbance of the Earth's natural magnetic field originating from a ferromagnetic object. They characterize various objects, but in this article, ships are taken into consideration. The signature can be measured without the knowledge of the measurement on the object being measured. Ships signatures can be used to analyze entries and exits from ports and passages through straits. By analyzing the magnetic signatures, one can infer the size and nature of the ship. In military applications, the magnetic signature of a ship is one of the criteria for mine activation.

Measurement of signatures conducted in a polygon is usually carried out under ideal technical, environmental and weather conditions. Therefore, these signatures are determined with high accuracy. However, when measuring devices are placed, for example, at the entrance to a port, the measurement is exposed to a number of interfering factors such as the ship's changing course, passing by magnetometers, the influence of other objects, large waves due to poor weather conditions, etc. In such cases, the determined signature is reproduced with high uncertainty. Due to the impact of the hull on waves and possibly on the quay during mooring, the permanent magnetization of the ship changes, thus the signature changes over the object's usage time relative to the measured signature. Also during mathematical modeling, certain simplifications of the object relative to the original are made, which also affects the shape of the signatures. Therefore, there is a need to assess the compliance of the signature with the pattern and how accurately the currently measured signature corresponds to

The associate editor coordinating the review of this manuscript and approving it for publication was Jenny Mahoney.

the reference signature and to what extent it belongs to a particular group of objects in the classification problem. For this purpose, classical statistical indicators and metrics for evaluating distances between curves are usually used.

In this paper, an alternative approach is proposed, namely a deep neural network, which provides a wide variety of applications in terms of signal processing, e.g. classification or regression [1]. A characteristic feature of deep neural network is the ability to capture abstractions, detect higher-level features by analyzing complex patterns in large amounts of input data. The definitional capabilities of deep neural networks have significant potential in applications for assessing the degree of compliance and membership in the appropriate predefined group or for identifying groups from the entire population. An approach of using them to classify ships' magnetic signatures is proposed, depicted with an example application of a deep, recurrent neural network with a GRU (Gated Recurrent Unit) layer for classifying magnetic signatures of ships' simplified models based on their proximity to the original signal, and a shallow one for classifying them by their size and type. Marine objects are classified based on various physical fields, such as magnetic, hydroacoustic, electric, hydrodynamic, and thermal. While data fusion techniques are typically used to enhance classification quality, this article focuses solely on magnetic signatures. The approach described has universal features that can be applied to other fields.

The authors plan to use the developed signature compliance classifier to assess model quality. Ship signature models can be created using forward and reverse approaches. In the forward approach, FEM class software is used to input details about the ship's structure, such as size, shape, material, and magnetic properties, to create an induced magnetization model. This model's accuracy is then compared to measurement data using the classifier to improve its fidelity. The reverse approach involves recording measurements and using them for machine learning model training and validation, with validation performed using cross-validation. The classifier also helps simplify FEM models, balancing between model quality and computation time by controlling the extent of simplification and assessing any resulting degradation.

Goal of the paper - to develop a new alternative to classical (based on statistical indicators) magnetic signature compliance classifier and to present a classifier for ships based on their type and size using their magnetic signatures. The need arose from related works concerning FEM and measurement-based modeling and simplification of the magnetic signatures.

Original contribution - After examining the literature no such application of classifying magnetic signatures based on their conformity with the original was found, and to author's knowledge it is a novelty. Necessary steps to develop a neural classifier were data collection and augmentation, finding the right ANN structure as well as its hyperparameters and reacting to arisen problems. M. Wołoszyn developed the ship models in the FEM environment for use as reference data for synthetic magnetic signatures, while methods for generating large sets of magnetic signatures for training purposes and finding the best neural network structure for the given task were achieved by Zielonacki and Tarnawski.

The paper is organized as follows: Section II provides a brief overview of the related works and the current knowledge on the subject. Section III contains an description of a multi-dipole model for predicting the magnetic signature, describes the process of generating training data for the learning process by modifying magnetic moments of the dipoles, and also shows the process of finding the best structure of the network for the task as well as the description of how hyperparameters were tuned, along with the training and test results. Section IV shows the process of generating magnetic signatures of a given ship's type in a given range of its length using interpolation, which then were used as input data for the classifier, whose structure and hyperparameters were also optimized. Finally, section V concludes the paper.

II. STATE OF THE ART

Recurrent neural networks, a class of neural networks designed for sequential data processing, have gained widespread attention in various domains. One of the seminal architectures in this category is the Long Short-Term Memory (LSTM) network, developed in 1997 [2], and can be frequently found in papers on classifying electroencephalogram (EEG) signals [3], text [4] and images [5]. In [6] the reader can find a comprehensive overview of the LSTM structure and applications. Gated Recurrent Unit, first proposed in 2014 [7] was designed to address some of the limitations of the LSTM architecture, such as computational complexity and vanishing gradient issues, while still maintaining its ability to capture long-term dependencies in sequential data [8] and has also been used in a wide range of applications, e.g. time series forecasting [8], where it outperformed LSTMs, machine health monitoring systems [9] and emotion classification [10].

Machine learning has also been used in the means of modelling the Earth's magnetic field [11]. An interesting example is the method described in [12], where a deep neural network with ReLU layers was used for modeling magnetic dipoles with very high accuracy. Other applications include predicting magnetic signatures [13], [14], as well as solving inverse-modeling problems [15], [16], [17], and metal detection tasks [18]. Another interesting application of neural networks and machine learning in combination with magnetic sensors is magnetic field-based indoor localization. The article [16] addresses the issue of locating an object inside a cube with sides of 2 m. The author compares the approaches of the k-nearest neighbor algorithm (k-NN) and artificial neural networks (ANNs) with modification for machine learning. The ANN approach is characterized by excellent achievements in the field of localization accuracy and is fast enough (while the network training time is relatively long)

that it can be used in real-time. Another application of ANN and magnetic signals concerns hand gesture recognition [19]. The authors present a hand glove with 6 nodes equipped with magnetic sensors. A Convolutional Neural Network is applied to gesture recognition. The authors achieved a correctness level of 93% among 26 gestures defined by the American Sign Language alphabet. In [20], the authors used a deep, residual, convolutional neural network for detecting magnetic anomalies and reached a very high accuracy despite high signal-to-noise ratio. In [21], authors provide an in-depth analysis of ANNs and random forests in maritime, offshore and oil and gas corrosion research in the years 2018-2023. They critically evaluated machine learning algorithms applied to maritime steel structures, pipelines, and construction materials, offering a valuable review for developing cost-effective maritime corrosion maintenance strategies. This work provides concise corrosion management expertise to empower both researchers and industry experts. The article [22] addresses the problem of minimizing the magnetic signature using Machine Learning techniques. The values of ampere-turns of coils placed in two variants inside and outside the simulated object with shapes corresponding to a submarine are determined. To deal with over determination and multicolinearity issues, the authors use the L2 (Ridge) regularization approach. The presented method is characterized by high degree signature silencing and computational efficiency that allows it to be used in real time. Similar issues related to the minimization of magnetic signatures were also considered by the authors of this article in [23] and [24] for arbitrary objects and in [25] for ships. Article [13] explores a genetic neural network approach, combining genetic algorithms with BP neural networks, to accurately predict the induced magnetic signature of ferromagnetic vessels, addressing limitations of traditional geomagnetic simulation methods. Similarly, Article [26] investigates the use of neural networks in underwater recognition systems, specifically focusing on the correlation between ship acoustic and magnetic fields. The study introduces the concept of a ship M-S diagram and demonstrates the effectiveness of a neural network model in achieving high recognition accuracy across different ship types. In [27] the authors further extend the application of neural networks by developing a model that predicts the external magnetic field in the closed-loop degaussing of ships. To overcome challenges related to insufficient training data, a data augmentation method is proposed, enhancing both the speed and accuracy of the model. Collectively, these studies underscore the potential of neural networks in improving the accuracy and efficiency of ship magnetic signature prediction and recognition systems. The issue of modeling magnetic signatures using neural networks has also already been addressed by the authors in [28], where a neural network was used to predict the magnetic signature depending on the measurement depth.

A common application of magnetism-related neural networks is classification. For example, in [29] the authors used a feedforward neural network to classify ship types. To achieve shorter calculation times, reduction methods were used. A comparison of backpropagation algorithms and genetic algorithms for training a neural network was conducted. In the article [30], a soft voting ensemble method using a deep learning classifier (for STM, GRU, and VGG16) was used, obtaining an f-score of over 90% for three classes of road traffic objects. Other classification examples include synchronous machines [31], mineral exploration [32] as well as different magnetic structures recognition [33].

The most frequently found method of assessment of ship's magnetic signature compliance is mainly centered around calculating the Root Mean Square Error (RMSE) or Mean Absolute Error (MAE) [34], [35]. Based on the literature analysis, the authors will propose a novel approach for assessing the conformity of signatures using deep learning with GRU layers, in the article.

Table 1 contains a comparison of other authors' work regarding the datasets ang algorithms they used, performance, advantages and limitations of the model. It can be seen that the datasets vary from application to another, but neural networks prove to be a reliable tool in classification or other problems, achieving high performance results. The dataset, however, often needs to be highly populated with well diversified data.

III. SIGNATURE COMPLIANCE CLASSIFICATION

This section discusses the classification of ship magnetic signatures based on their compliance with the reference. It explores the process of creating training data, selecting suitable network structure and adjusting settings for better performance.

A. THE TRAINING DATA

1) MAGNETIC SIGNATURES AND MULTI-DIPOLE MODEL

A magnetic signature is a mathematical description of a ship's disruption of the Earth's magnetic field [36]. This description can be approximated using a multi-dipole model [37], [38], which describes the i-th dipole at an arbitrary position (x, y, z) with a vector of magnetic flux density as follows [39], [40]:

$$\mathbf{B} = \sum_{i=1}^{m+n} \mathbf{B}_i(\mathbf{M}_i, \mathbf{R}_i) = \sum_{i=1}^{m+n} \frac{\mu_0}{4\pi} \cdot (\mathbf{R}_i^T \mathbf{M}_i \mathbf{R}_i \cdot \frac{3}{R_i^5} - \frac{\mathbf{M}_i}{R_i^2}) \tag{1}$$

$$\mathbf{B} = \begin{bmatrix} B_x \\ B_y \\ B_z \end{bmatrix}, \mathbf{B}_i = \begin{bmatrix} B_{x,i} \\ B_{y,i} \\ B_{z,i} \end{bmatrix}, \mathbf{M}_i = \begin{bmatrix} m_{x,i} \\ m_{y,i} \\ m_{z,i} \end{bmatrix}, \tag{2}$$

$$\mathbf{R}_i = \begin{bmatrix} (x - x_i) \\ (y - y_i) \\ z_i \end{bmatrix}, R_i = |\mathbf{R}_i|, \tag{3}$$

where $\mathbf{B}$ is the magnetic flux density vector, m is the number of permanent dipoles, n is the number of induced dipoles, $\mathbf{B}_i$ is the magnetic flux density vector of i-th magnetic dipole, $\mathbf{M}_i$ is the vector of the magnetic moments of i-th dipole and

TABLE 1. Comparison of other authors' work.

Quotation	Dataset	Algorithm	Performance	Advantages	Limitations
[11]	Earth's magnetic field measurements from three months	ANN model with sigmoid activation functions	Efficient, based on absolute error values and correlation between modeled and observed values	Quick model construction, prediction of unseen examples	Closed-box nature of the model, computational burden, empirical nature of the model
[12]	10 000 pairs of magnetic induction data and dipoles' parameters	Deep ReLU network	Reproduction with relative deviation lower than 2%	Accurate prediction of the magnetic source parameters	Not stated
[14]	16 380 magnetic data maps	CNN	Prediction of the angle of inclination and declination with at most 1 angle category difference	Body shape, size and thickness do not significantly affect the prediction, robustness against different assumptions of depths	Depth and lateral positions of the source body affect the prediction
[16]	3 306 038 TX states	ANN model	Achieving prediction error lower than 0.1 m 97.2% of the time	Prediction time allows for real-time tracking	Longer to train than k-NN
[19]	1 200 data points for 26 gestures of letters with 18 magnetic field data points each	1-D CNN	97% accuracy of classification	Increased accuracy in recognition and immunity to environmental interference when compared to traditional gesture recognition technology	Not stated
[20]	13 000 background magnetic fields	Deep CNN	98.8% classification accuracy	Best accuracy of all compared methods	Not stated
[33]	50 000 images of magnetic fields	Deep CNN	85.68% validation accuracy	Lightweight model	Lower accuracy when compared to pre-trained models

$\mathbf{R}_i$ defines the distance between the i-th dipole and the analyzed point.

A 25-permanent and 25-induced dipole model was developed in MATLAB using synthetic data from a ship model constructed in Simulia Opera 3D [41] environment (detailed description of which can be found in the appendix) and an optimization method described in [34], which finds the positions and moment values of each dipole in the model that best fit the reference data in port (P), keel (K) and starboard (S) lines (see figure 1).

The objective function for m permanent and n induced dipoles given by:

$$\min_{\Omega\in\{\Omega_1,\ldots,\Omega_{n+m}\}} J = \sum_{l}\sum_{k}\sum_{d}\sum_{j=-300}^{300}(\mathbf{B}_{l,d}^{ref}(j,k) - \mathbf{B}_{l,d}^{model}(j,k,\Omega)^2) \tag{4}$$

$$\text{s.t. } \forall i \in (1, m+n)\ \Omega_i^{min} \leq \Omega_i \leq \Omega_i^{max} \tag{5}$$

where

$$\text{s.t. } \forall i \in (1, m+n)\ \Omega_i \in \{m_{x,i}, m_{y,i}, m_{z,i}, x_i, y_i, z_i\}, \tag{6}$$

$$l \in \{x, y, z\} \tag{7}$$

$$k \in \{P, K, S\} \tag{8}$$

$$d \in \{0^o, 90^o, 180^o, 270^o\} \tag{9}$$

and Ω_i^{min} Ω_i^{max} define the optimization search space. Figure 2 is a visualization of the dipoles' locations.

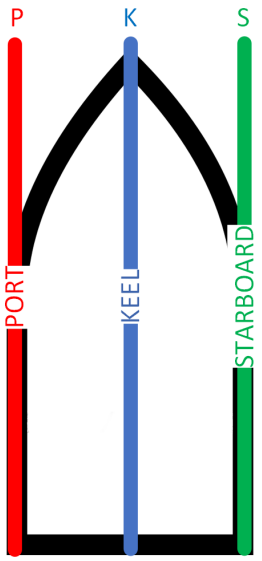

FIGURE 1. P, K and S lines locations.

Using this model, the magnetic flux density along the keel path can be determined in each direction: north, west, south and east, and for all cartesian directions (x, y and z), resulting in graphs shown in figure 3, along with the reference data.

The RMSE between the model and the reference data is equal to 0.3446, which means a very good fit. This model will now be taken as a reference for further investigation.

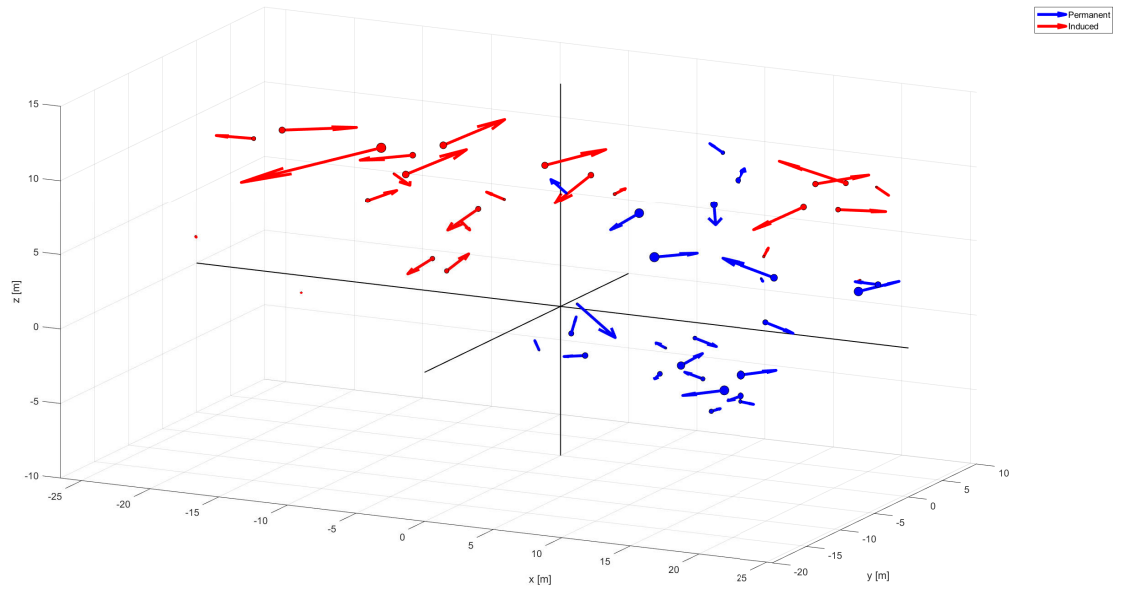

FIGURE 2. Locations and magnitudes of dipoles.

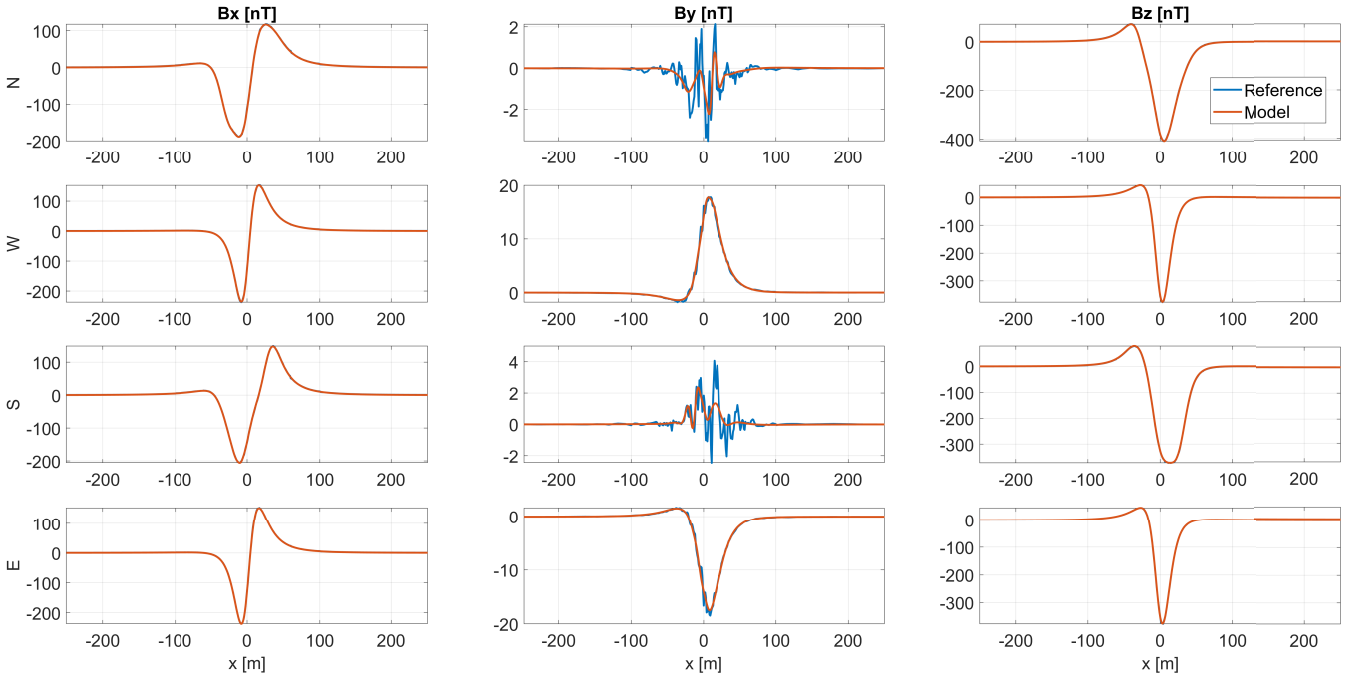

FIGURE 3. Keel path - model and reference.

2) GENERATING MODIFIED MAGNETIC SIGNATURES

In order to train a neural network, a large dataset is necessary to obtain satisfactory results. To achieve that, magnetic moments of the multi-dipole model were disturbed by maximum of 1% with a step of 0.001%, creating a new dataset of signatures differing from the reference one. Figure 4 shows an example heatmap of 10000 signatures gathered by altering the moments with a 0.5% normally distributed disturbance, where yellow color indicates that most of the signatures were following that path.

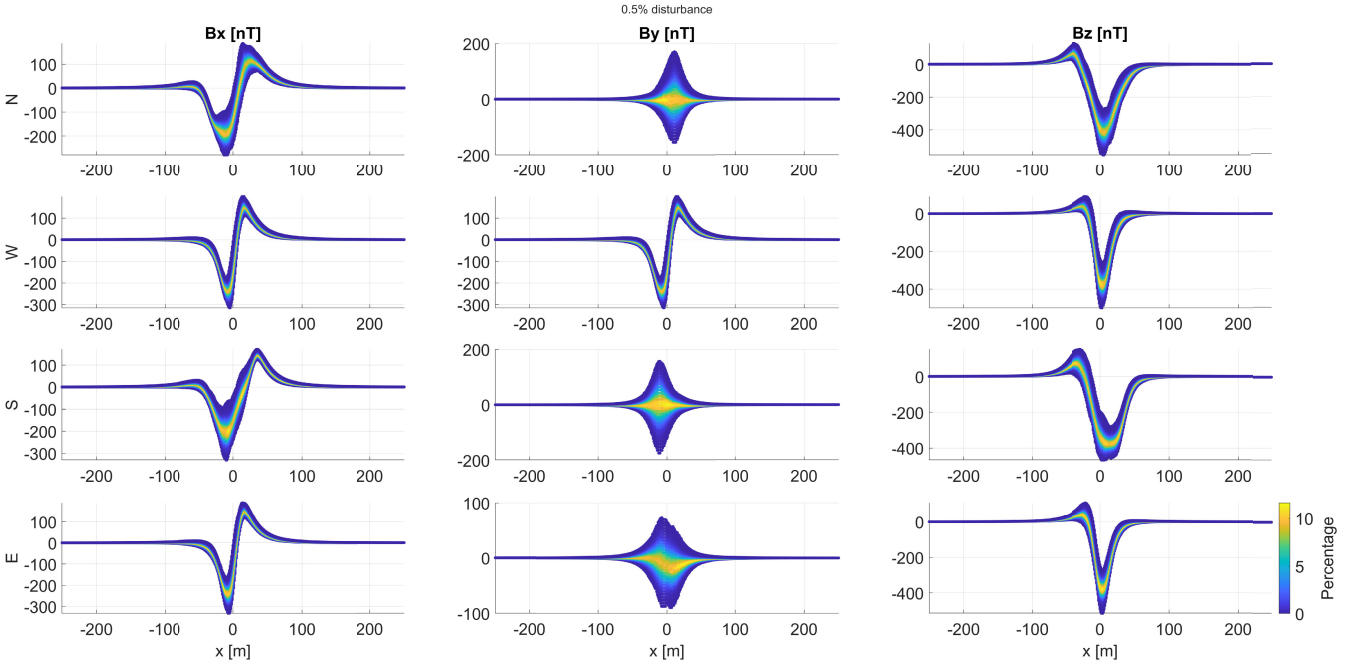

FIGURE 4. Heatmaps of 10000 signatures generated by 0.5% magnetic moment disturbance.

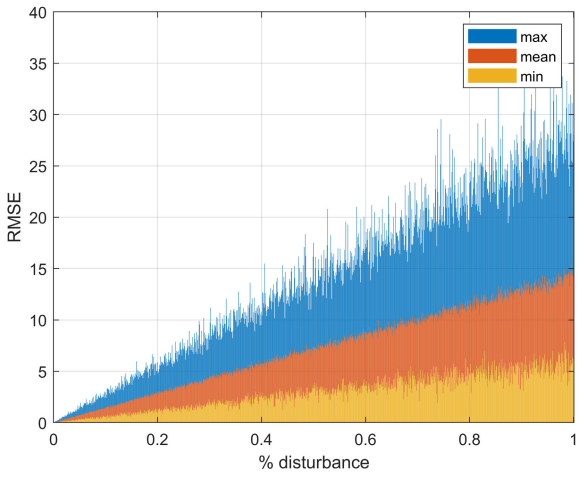

FIGURE 5. RMSE distribution.

This method of generating different magnetic signatures allows to obtain a sparse dataset with different error values, which are necessary to assess their compliance. Figure 5 shows how the mean, maximum and minimum values of RMSE between the reference signal y and the disturbed signal y_d given by (10) are distributed depending on the disturbance magnitude.

$$RMSE = \sqrt{\sum_{i=1}^{N} \frac{(y[i] - y_d[i])^2}{N}} \tag{10}$$

Judging from the plot, the class of 0% compliance was assigned to all signals with RMSE larger than 15, as this was the mean value of RMSE for the biggest disturbance, and this range is determined to be the working range of applicability for the classifier. Then, subsequent classes were assigned linearly with a 10% step, meaning that RMSE ranging from 13.5 to 15 was a 10% compliance class, 12 to 13.5 a 20% compliance class etc, resulting in 11 classes in total. This choice, however, comes only from the fact that 1% disturbance of dipoles' moments results in approximately 15 nT RMSE in the data. The choice here is arbitrary and the user can scale the compliance intervals differently (it is a tuning parameter of the method). The dataset consisting of 100000 sequences was partitioned into 80% training data, 10% validation data and 10% test data.

B. NETWORK STRUCTURE, TRAINING AND HYPERPARAMETER TUNING

1) GRU ARCHITECTURE

The GRU represents a specialized architecture within RNNs, devised to address the limitations of traditional neural networks in modeling long-term dependencies in sequential data. It contains gating mechanisms that regulate the flow of information through the network, enabling adaptive memory management and enhanced learning capabilities. The GRU architecture consists of two main gates: the update gate and the reset gate. The relationship between input and output at time t can be described as follows:

$$z(t) = \sigma(\mathbf{W}_z x(t) + \mathbf{U}_z h(t-1) + b_z \tag{11}$$

$$r(t) = \sigma(\mathbf{W}_r x(t) + \mathbf{U}_r h(t-1) + b_r \tag{12}$$

$$\hat{h}(t) = tanh(\mathbf{W}_h x(t) + \mathbf{U}_h(r(t) \odot h(t-1) + b_h) \quad (13)$$

$$h(t) = (1 - z(t)) \odot h(t-1) + z(t) \odot \hat{h}(t) \quad (14)$$

where $x(t)$ is the input vector, $z(t)$ is the update gate output, $r(t)$ is the reset gate output, $\hat{h}(t)$ is the hidden state candidate, $h(t)$ is the output vector, $\mathbf{W_z}$, $\mathbf{W_r}$, $\mathbf{W_h}$, $\mathbf{U_z}$, $\mathbf{U_r}$ and $\mathbf{U_h}$ are weight matrices, b_z, b_r and b_h are bias terms. σ denotes the sigmoid operation and $\odot$ is the piecewise multiplication operator.

2) FINDING THE BEST STRUCTURE

For the classification task, the main performance indicator of the neural network is classification accuracy, which is defined as the ratio of the number of correct predictions made by the model to the total number of predictions.

Shallow neural network did poorly with the task at hand, achieving maximum accuracy of 40 %. After a few tests, the best initial results were obtained with a network that had five hidden layers. The network structure chosen for the task and written in MATLAB using the Deep Learning Toolbox [42] consists of 7 layers:

- the feature input layer, where each of the 12 paths with 501 data points is passed through, resulting in 6012 neurons,
- five hidden layers,
- and a classification layer.

Also, for regularization purposes, batch normalization layers after each activation layer and two dropout layers were added.

In order to find the best structure for the hidden layers, a method of hyperparameter optimization called grid search [43] was used. An algorithm was developed, where each of 32 possible structures was represented in binary code, e.g. 00101 is represented with a number 5 and means the first and the third layers are GRU and the second, fourth and fifth is ReLU (Rectified Linear Unit). The number of neurons in each layer was randomly selected from the set $\{8, 16, 32, \ldots, 1024\}$, and the model was trained using Adam optimization algorithm with 0.001 learning rate and a mini-batch size of 256, with maximum number of epochs equal to 100 and the validation patience of 10, allowing epochs not to be of concern. Also, the returned network for each training was the one with the lowest validation loss. Gradient threshold was set to 1 to ensure stability. The test was repeated five times for each variant. Figure 6 shows the results of the search, with the variants on the x-axis and the test accuracy on the y-axis.

Interestingly, every second variant showed good results, while other were very inaccurate. This suggests that GRU cannot be the first layer, since in each of these variants it was. The best structure, which was variant 8 with the set of neurons of {64, 1024, 64, 32, 32} was selected for further tuning.

Next, using the same grid search method, the best optimization algorithm, learning rate and batch size was selected. Three algorithms were considered: Adam, SGDM and RMSprop. The learning rate was selected from the set $\{0.1, 0.01, 0.001, 0.0001\}$, and the batch size from the set $\{64, 128, 256, 512, 1024\}$. The number of epochs and validation patience remained the same. Table 2 shows the results of the search, where the accuracy is given for each hyperparameter configuration, with the best result marked in bold.

TABLE 2. Results of the algorithm and learning rate grid search.

Adam						
Learning rate	Batch size					
	128	256	512	1024	2048	4096
0.1	0.5007	0.6283	0.6767	0.7806	0.8195	0.8310
0.01	0.5791	0.6883	0.8400	0.8399	0.8791	**0.8965**
0.001	0.6677	0.7037	0.6141	0.5232	0.4827	0.4353
0.0001	0.3544	0.4508	0.5671	0.4956	0.4948	0.4745
SGDM						
Learning rate	Batch size					
	128	256	512	1024	2048	4096
0.1	0.6497	0.7683	0.7318	0.5828	0.5218	0.4576
0.01	0.5046	0.4655	0.4360	0.4816	0.4085	0.5198
0.001	0.2497	0.3785	0.4201	0.4508	0.5670	0.6095
0.0001	0.2634	0.3617	0.4825	0.5309	0.4562	0.4421
RMSprop						
Learning rate	Batch size					
	128	256	512	1024	2048	4096
0.1	0.3502	0.5165	0.4881	0.5630	0.5825	0.6167
0.01	0.6596	0.6730	0.6826	0.8170	0.8508	0.8412
0.001	0.5984	0.7553	0.7332	0.6734	0.7123	0.6677
0.0001	0.3131	0.5139	0.4538	0.5419	0.4599	0.6228

TABLE 3. Results for different number of classes.

Error step	Number of classes	Accuracy
10	11	0.953
5	21	0.8903
4	26	0.8720
2	51	0.8516
1	101	0.7009

Finally, the best number of neurons in each layer was found. Because the configuration space in this case is large, the method of random search was used. The values were selected from the set $\{8, 16, 32, \ldots, 4096\}$ randomly for 30 iterations, and the resulting numbers of neurons were as follows: {1024, 2048, 128, 128, 128, 4096} for each layer respectively. Figure 7 shows the learning curves of the net. It had the test accuracy of 0.9173.

After examining the plot, it was decided to increase the maximum number of epochs to 200 since the last validation performance was the best and also use a piecewise learn rate schedule, where learning rate was multiplied by 0.5 every 20 epochs. The final achieved test accuracy was 0.953. Figure 8 shows the confusion matrix of the trained network.

The network has demonstrated satisfactory performance, achieving a high level of accuracy. Moreover, when it assessed the compliance of a magnetic signature incorrectly, it was only off by one degree. The net was also tested when it was attempted to classify more compliance classes. The tested error steps were 10%, 5%, 4%. 2% and 1%. Table 3 shows the results of that experiment for different numbers of classes. As expected, the increase of the number of classes causes test accuracy to deteriorate. However, even in the last case, the classifier was off by a maximum of three classes.

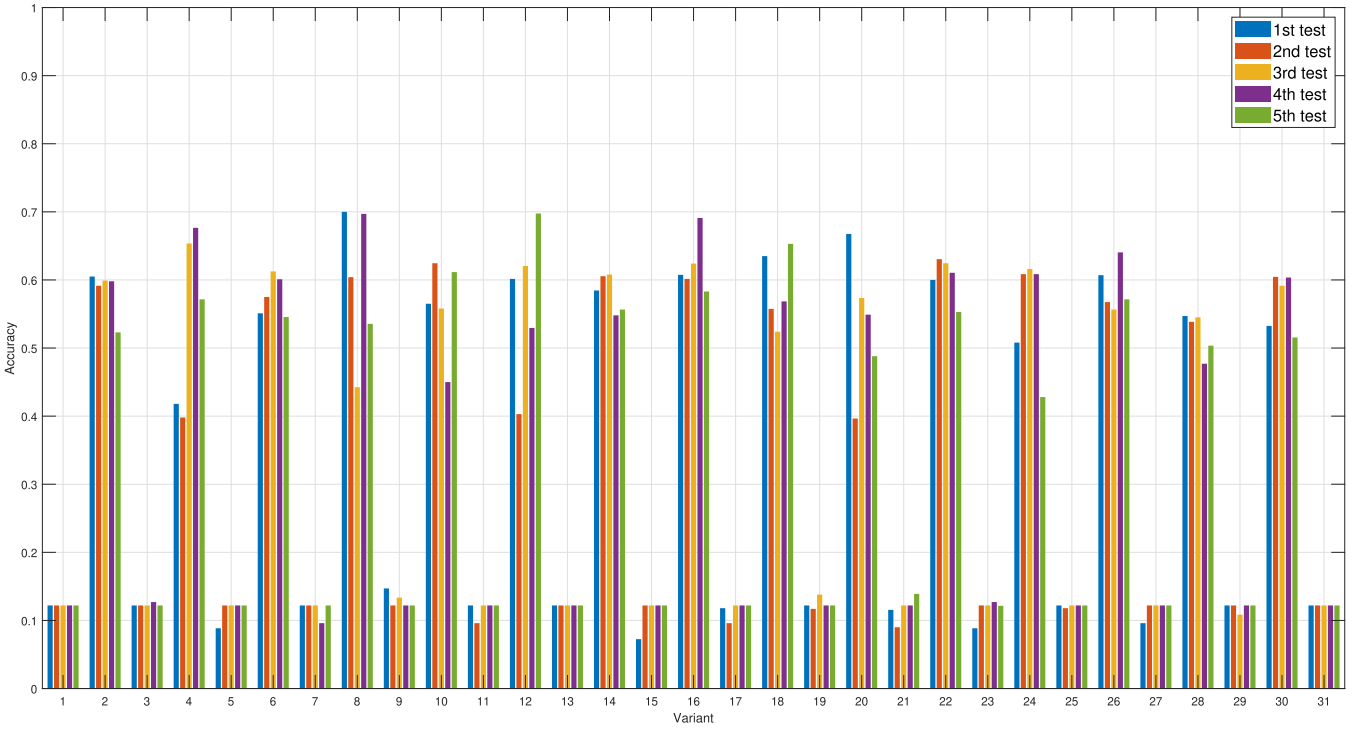

FIGURE 6. Results of the structure grid search.

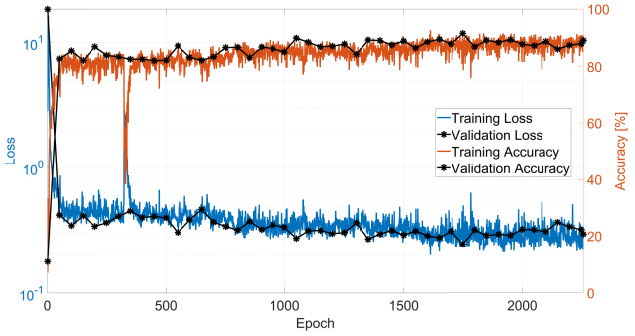

FIGURE 7. Learning curves of the network.

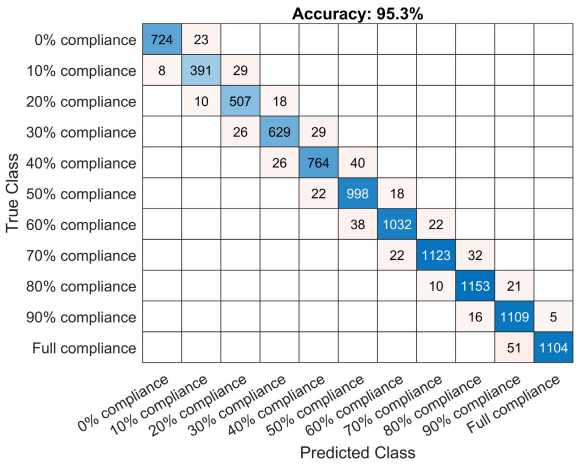

FIGURE 8. Test confusion matrix.

C. VERIFICATION

The classifier was verified using signatures coming from a different kind of disturbance - a new induced dipole with uniformly-distributed random moments values, that ranged from the minimum value of the reference model's moments to the maximum, multiplied by a scaling factor, was added to the multi-dipole model, causing anomalies in the plots. In order to remain in the 0-15 range of RMSE, the scaling factor of the extra dipole was set to be in range 0.001-0.1, which was confirmed experimentally. Figure 9 shows how the mean RMSE values were distributed across the set of 100000 signatures.

Figure 10 shows example signatures, where the scaling factor is equal to 0.05. As can be seen in the figure, the disturbance mostly alters the signatures in the B_y component in north and south directions. This method allowed to create a new test set of signatures of a kind that the classifier had not seen before.

The verification set was then inputted to the classifier. Figure 11 shows the confusion matrix for the new test data.

As expected, the network properly classified signatures, where the compliance was one hundred percent. However, it poorly recognized all the other data, where the RMSE was higher than 1.5. Poor performance is most likely caused by disturbances coming from a different source, causing them not to be recognized by the classifier.

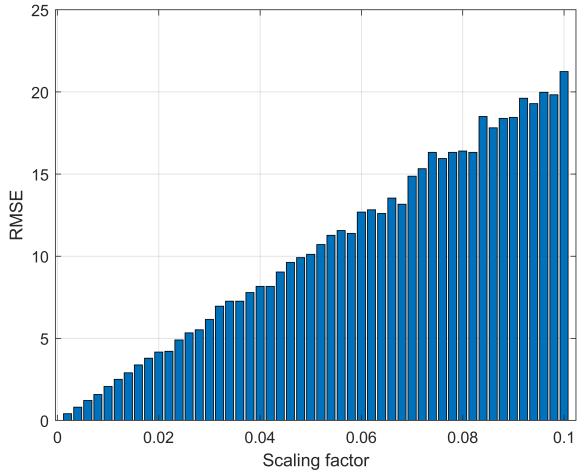

FIGURE 9. Mean RMSE distribution of signatures coming from multi-dipole models with an additional disturbance induced dipole.

TABLE 4. Results for different number of classes.

Error step	Number of classes	Accuracy
10	11	0.8990
5	21	0.8152
4	26	0.7525
2	51	0.6996
1	101	0.4951

D. IMPROVING THE CLASSIFIER

Poor test performance was addressed by adding the data coming from models with additional dipole to the training set. Options for the training and the network structure remained equivalent to the ones used previously. Table 4 shows the test results for different numbers of classes, while Figure 12 depicts the confusion matrix for 11 classes. It can be seen, that although with a slightly lower accuracy, the classifier is able to return accurate information about signatures' degradation proportionally to its deformation. Even in the last case for 101 classes, where the accuracy was lower than 50%, the error was not larger than 5 degrees of compliance. Nevertheless, the case where each class is one percent, the regression task would be more appropriate.

E. CLASSIFIER BASED ON MAE

Another way of assessing the compliance of a signal is with MAE, given by (15). A training dataset was generated using the same methods described previously, with MAE indicators being assigned to them as target values. Figure 13 shows the distributions of the errors for disturbances of dipoles' models, while figure 14 shows the mean distributions of the errors for models with an additional disturbance induced dipole. Lowest class of compliance was assigned to signatures with MAE higher than 5, and the rest was assigned linearly, in the same fashion as the previous classes.

$$MAE = \sum_{i=1}^{N} \frac{|y[i] - y_d[i]|}{N} \tag{15}$$

As previously, the dataset was divided into 80% training, 10% validation and 10% test data. For 11 classes, the accuracy was equal to 88.9%. The working principle of the network is the same as previously, so the accuracy is also high in this case. Figure 15 shows the confusion matrix for 11 classes based on MAE and table 5 shows the results for different number of classes.

TABLE 5. Results for different number of classes based on MAE.

Error step	Number of classes	Accuracy
10	11	0.8890
5	21	0.7822
4	26	0.7264
2	51	0.6712
1	101	0.5197

F. INFLUENCE OF DATASET SIZE ON PERFORMANCE AND TRAINING TIME

A dataset size of 100 000 samples was chosen arbitrarily and it was decided to analyse the influence of the number of samples in the training set on the performance of the network. It is well known that the dataset size can significantly influence the training time and its computational burden [44], [45]. The training process was repeated for different numbers of signatures and each time the set was divided the same way as before, into 80%, 10% and 10% of training, validation and test data respectively. Figure 16 shows the results of the experiments, where the accuracy and training time was depicted. Each time the network was trained for the RMSE case with 11 classes.

The plot illustrates the relationship between the number of training samples, model accuracy, and training time. As the number of training samples increases, model accuracy generally improves, particularly in the early stages, where significant gains are seen up to around 30,000 samples. Beyond this point, accuracy continues to rise but at a slower and more fluctuating rate, indicating diminishing returns as the dataset size grows. Training time, on the other hand, increases nearly linearly with the number of training samples, reflecting the higher computational demand. This relationship highlights a trade-off: while larger datasets enhance accuracy, they also significantly increase training time. Notably, after a certain threshold (around 50,000 samples), the accuracy gains become minimal. When it comes to performing a single classification, on average it took 132 μs.

IV. SHIP SIZE AND TYPE CLASSIFICATION

This section focuses on classifying ship size and type based on their magnetic signatures. The training data is prepared using numerical ship models and interpolation method. A single hidden layer GRU neural network is fine-tuned through grid search to achieve satisfactory results.

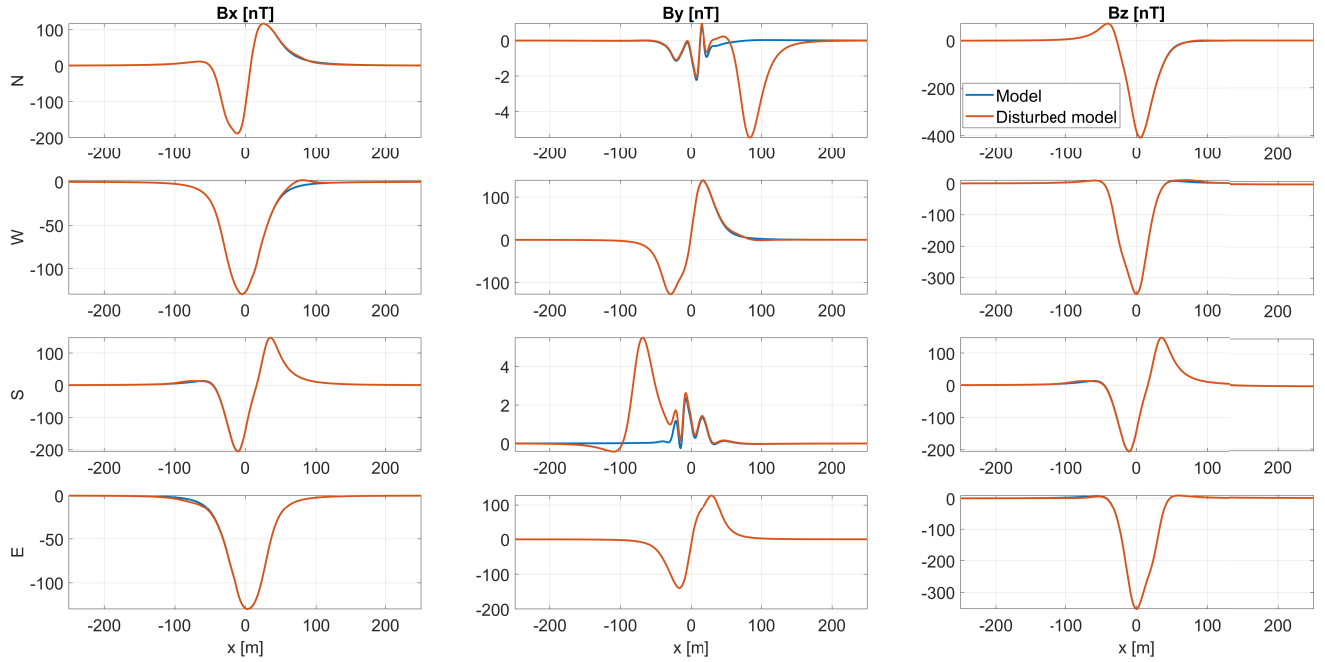

FIGURE 10. Magnetic flux of reference multi-dipole model and disturbed one with additional induced dipole.

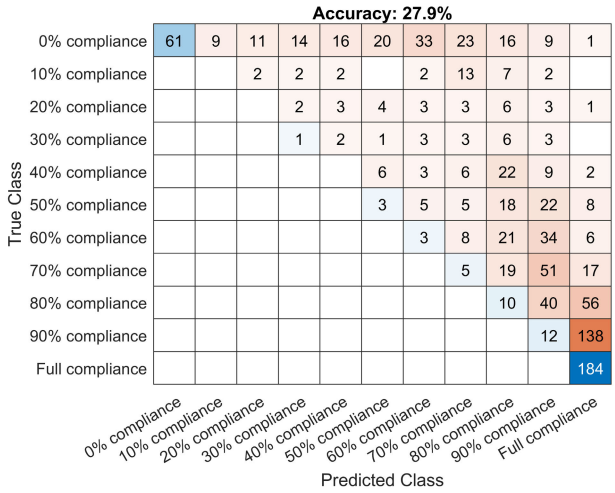

FIGURE 11. Verification confusion matrix.

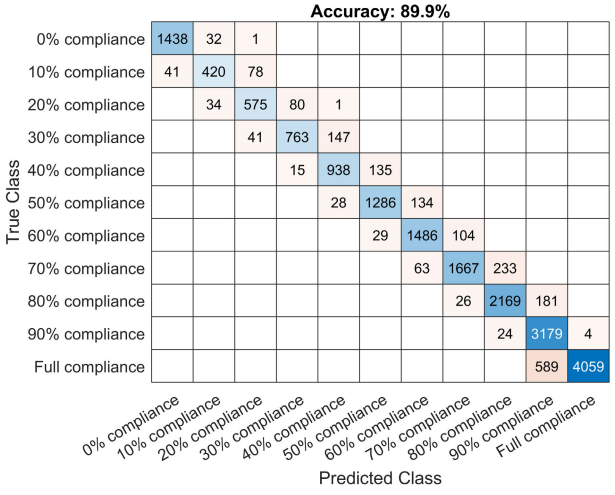

FIGURE 12. Verification confusion matrix after including the second test data.

A. THE TRAINING DATA

1) PREPARING THE MODEL

In the FEM Simulia Opera 3D software, two numerical models of ships with a length of 42 meters have been prepared, but with different sizes and shapes. The shape of the corvette is shown in figure 17a, and its magnetic signature at the measurement depth of 5 meters is shown in figure 18. This is the same model that was used for compliance classification. The shape of the tugboat is shown in figure 17b, and its magnetic signature at the measurement depth of 5 meters is shown in figure 19. The details on the FEM simulation of the tugboat are also included in the appendix.

Creating a numerical model of a ship is time-consuming, and it is difficult to assemble the entire fleet (provide so many different versions of ships) for the purpose of training neural networks and verifying the classifier. Therefore, it was decided to demonstrate the classification capabilities of these two types of vessels, but in different sizes. The FEM software allows for scaling of the developed object, thus several size versions of each of the two presented types of ships were created. Then, a scaling code for these signatures was developed for the desired size of the ship within a certain range. This way, any number of signatures for different ship sizes can be provided for the training dataset.

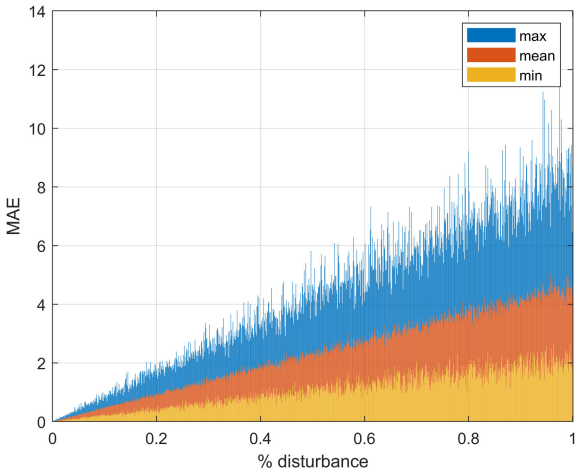

FIGURE 13. MAE distribution.

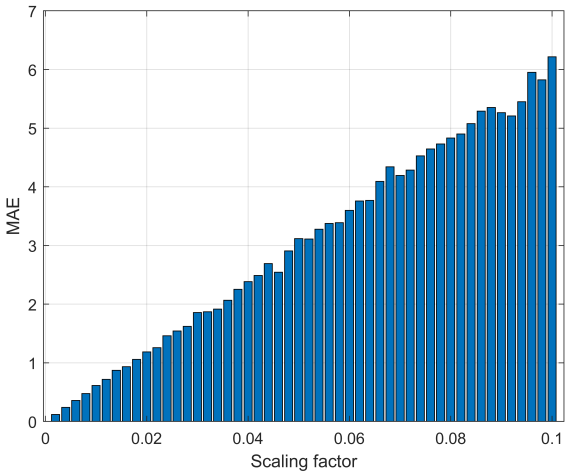

FIGURE 14. Mean MAE distribution of signatures coming from multi-dipole models with an additional disturbance induced dipole.

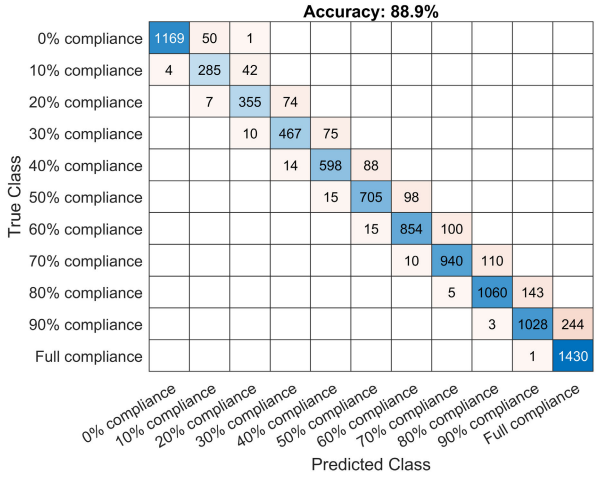

FIGURE 15. Test confusion matrix of MAE classifier.

2) A SIGNATURE GENERATOR FOR A GIVEN SHIP SIZE

At a measurement depth of 5 meters, the magnetic signatures presented in figures 18 and 19 still have irregular shapes.

FIGURE 16. Compliance classification results for different dataset sizes.

FIGURE 17. Ships' models.

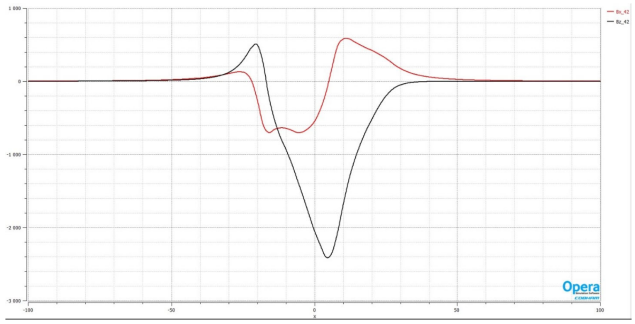

FIGURE 18. The corvette signature at a measurement depth of −5 meters.

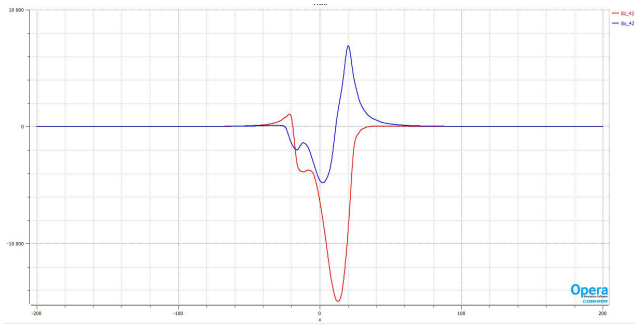

FIGURE 19. The tugboat signature at a measurement depth of −5 meters.

Moving away from the measurement devices to 10 meters results in the signatures having regular shapes, i.e., they do not differ in character depending on the size of the ship, and characteristic points can be identified in them. In figure 20, a family of signatures from a measurement depth of 10 meters is shown for corvettes of different lengths (42 m, 38 m,

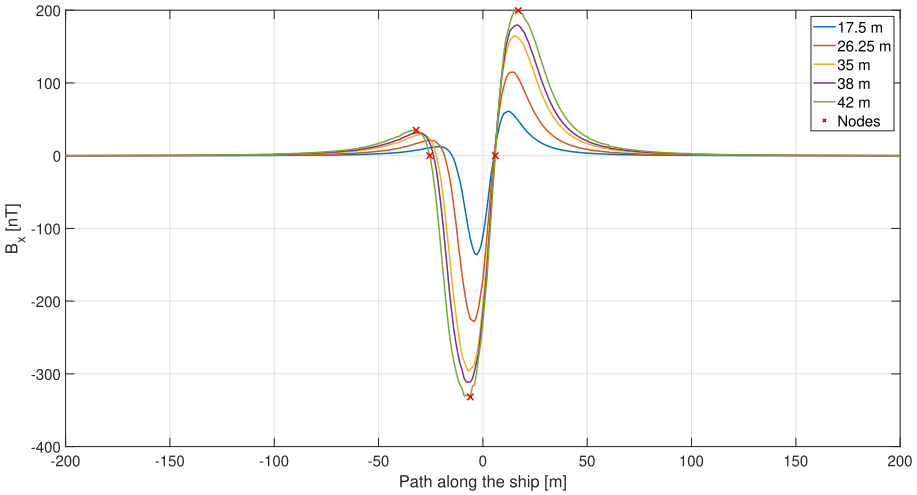

FIGURE 20. A family of signatures for the corvette ship with various lengths and marked key interpolation nodes.

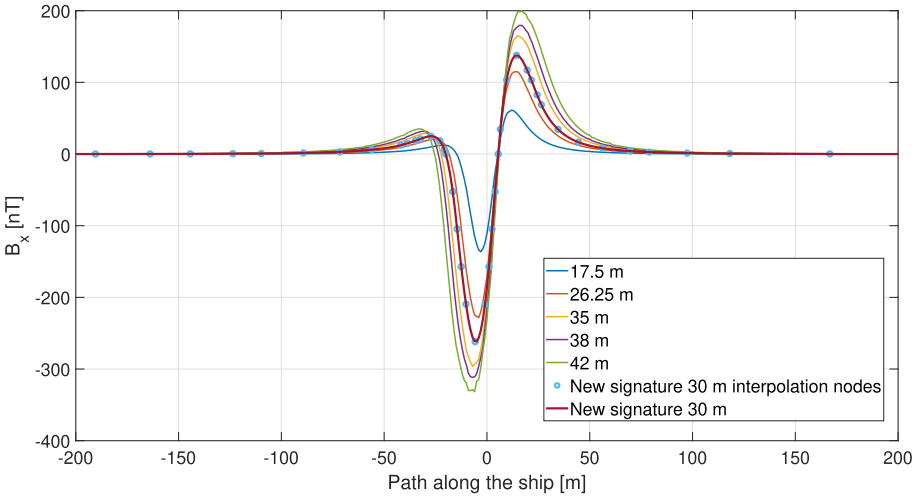

FIGURE 21. The generated signature for the corvette ship with a length of 30 meters.

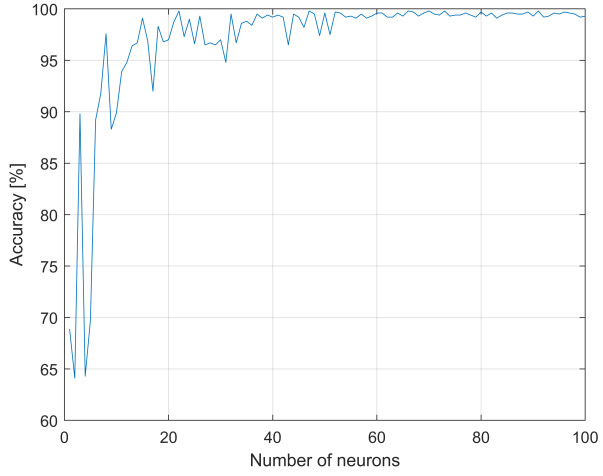

FIGURE 22. Grid search results.

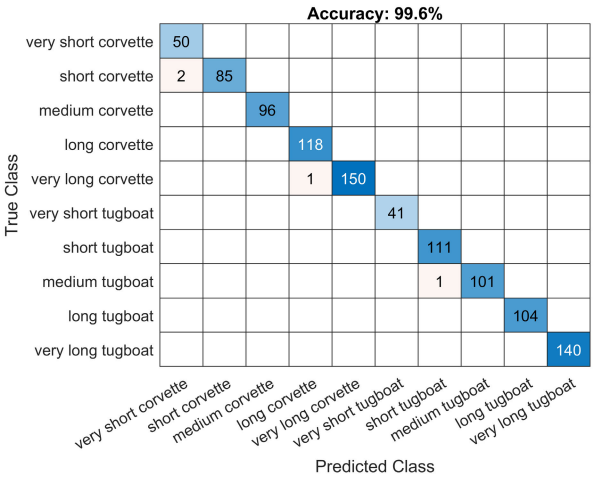

FIGURE 23. Test confusion matrix for classification of type and size.

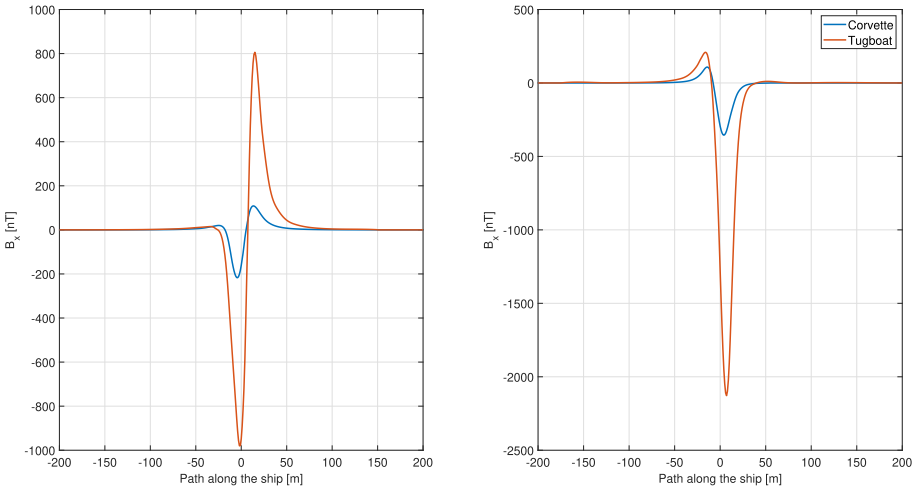

FIGURE 24. Reference signatures of the corvette and the tugboat.

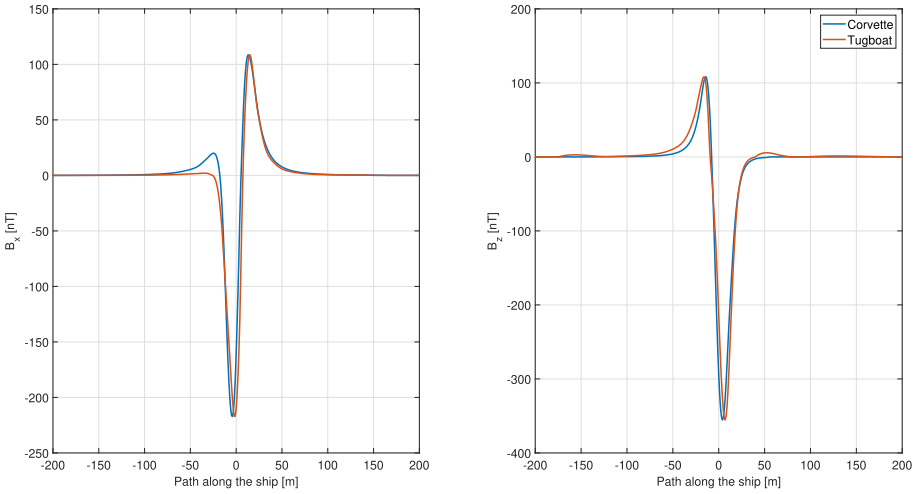

FIGURE 25. Scaled signatures of the corvette and the tugboat.

35 m, 26.25 m, 17.5 m). On the signature of a ship with a length of 42 m, characteristic points are marked: 1) local maximum, 2) first zero crossing, 3) minimum, 4) second zero crossing, 5) maximum. These points will serve as interpolation nodes, but they also allow dividing the B_x signature into 6 intervals, in which subsequent nodes are found, representing, for example, $\frac{1}{2}$, $\frac{1}{4}$, etc., of the maximum or minimum values. In total, each signature is described using 41 points.

Having the values of reference points of signatures for known ship lengths, interpolation of nodes can be performed for the signature of a virtual ship with a length ranging from 17.5 m to 42 m. After another interpolation, connecting the reference points, the entire signature can be obtained. The effect of this generator can be seen in figure 21 in the form of a created signature describing a corvette with a length of 30 m - not present in the FEM dataset.

The correctness of generating signatures of the specified length was verified using the Leave One Out Cross-Validation method by interpolating data for four lengths and finding the interpolated value of the signature for the ship length for which FEM data were available, e.g., interpolation data came from ships with lengths of 42 m, 38 m, 35 m, 17.5 m, and were verified using a size of 26.25 m. The proposed method was verified with high accuracy. The described approach was also applied to create B_z signatures of magnetic flux density and for a tugboat type ship.

An inevitable element of introducing an augmented approach by using interpolation in the process of creating a training dataset for a neural network is a potential bias that could affect the classification process. In order to assess its real impact, calculations using ideal data and interpolated data should be contrasted. This would require having either FEM or actual measured data from any available depth which is virtually impossible with real data. With this knowledge

TABLE 6. Summary of the classifiers' aspects.

Classification type	Dataset	Algorithm	Performance	Advantages	Limitations
Compliance	100 000 artificially generated disturbed magnetic signatures	GRU-based deep network	Over 90% accuracy for 11 classes	Quick classification, high accuracy, different quality indices	Large dataset, long training time, works still based on statistical indicators
Size & type	5 000 magnetic signatures of two types of ships each, for different sizes	One-layer GRU	Almost 100% accuracy for relatively low number of neurons in a single layer	Very high accuracy to complexity ratio	Need for data augmentation via interpolation

that measured data will only be available from a few depths, interpolation techniques have been proposed to augment the data for neural analyses. The impact of the interpolation is essentially the opening of another research issue and is not the direct purpose of this article The quality of the model created by the interpolation techniques used was good enough and verified with reference data that the errors from the interpolation used can be considered as either negligible or acceptable.

B. THE CLASSIFIER

Again in Matlab, a program was written for classifying the size and type of a ship based on its magnetic signature, using a generated dataset of 10000 signals. As before, this dataset was divided into 80% training data, 10% validation data, and 10% test data. After initial tests, it turned out that there was no need to use a deep neural network for this task, as a single hidden layer GRU already showed good results. In fact, these results were even better than when additional layers were added. To minimize the program, a grid search was conducted, the results of which are shown in figure 22. It can be noticed that already for 22 neurons, an accuracy higher than 99% was achieved. However, it can be observed that stable results were obtained above 52 neurons, mainly due to the use of the stochastic optimizer Adam, and for this value it was decided to create a classifier, whose final test accuracy reached 99.6%. Figure 23 shows the confusion matrix on the test set.

C. SCALING THE SIGNATURES

The results obtained in the previous subsection were exceptionally high, which was caused by the fact, that the tugboat's signatures were much bigger in magnitude than the corvette's, which is visualized in figure 24, where one can see how big the difference is. The decision was made to try giving the classifier a harder task, by artificially scaling the signatures to the same range, the result of which is shown in figure 25. This way, a new training dataset consisting of 10000 signatures in similar value range was created, and the classifier was tested again. Figure 26 shows the confusion matrix of the final test.

It can be seen, that despite scaling the signatures, a single-layer GRU network is more than capable of classifying ships by their size and type, achieving a remarkable 99,8% accuracy.

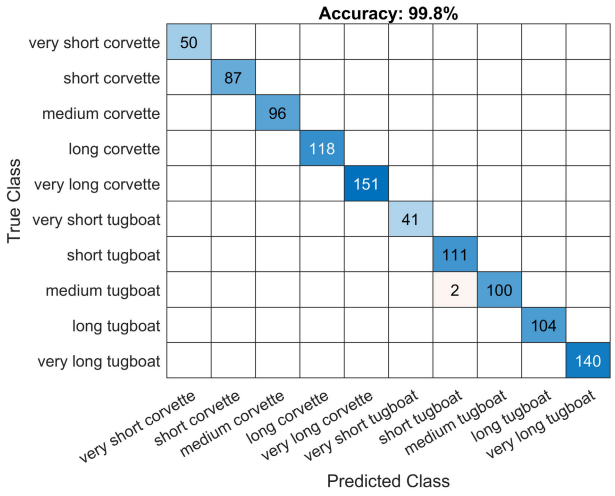

FIGURE 26. Test confusion matrix after scaling the signatures.

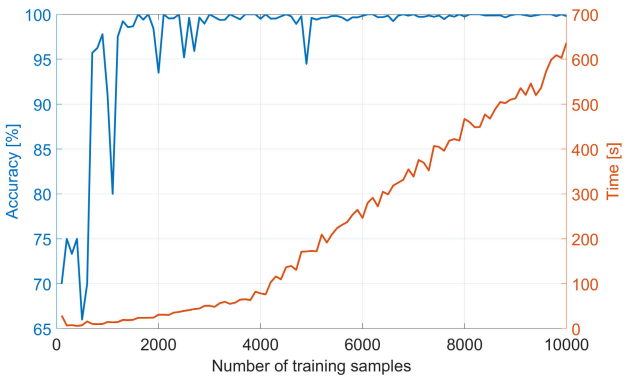

FIGURE 27. Size and type classification results for different dataset sizes.

D. INFLUENCE OF DATASET SIZE ON PERFORMANCE AND TRAINING TIME

Again, the choice of 10 000 samples as the size for the dataset was arbitrary and it was decided to analyze its influence on classification accuracy. As previously, the training process was repeated for different numbers of signatures and each time the set was divided the same way as before, into 80%, 10% and 10% of training, validation and test data respectively. Figure 27 shows the results of the experiments, where the accuracy and training time was depicted.

The number of 10,000 data assumed the first time proved to be redundant to sufficiently achieve satisfactory classification quality. Inferring from the graph, already with 1,300 samples, an almost 100 per cent efficiency can be achieved, while above 3,000 samples it is achieved steadily. As expected, the training time increases linearly with dataset size, although a slight increase in its slope can be noticed at 4000 samples threshold. When it comes to performing a single classification, on average it took 64 μs.

V. DISCUSSION AND CONCLUSION

In this paper, a novel approach of utilizing deep learning techniques for classifying ships' magnetic signatures and predicting their size and type was presented. The methodology involved the development and training of RNNs, specifically using GRUs, to handle sequential data effectively.

For the classification of compliance between original and modified magnetic signatures, a multi-dipole model was utilized to generate a diverse dataset. A deep RNN architecture with GRU layers was designed and optimized using grid search and random search methods for selecting the best network structure and hyperparameters. After including a disturbance of different type which shown to be impactful on the network's performance, the trained classifier demonstrated high accuracy in assessing the compliance of signatures.

Furthermore, a classifier was developed to recognize the size and type of ships based on their magnetic signatures. A signature generator was developed to create synthetic data for different ship sizes, enabling the training of the classifier. The GRU-based classifier achieved exceptional accuracy in classifying ship size and type.

After examining the performance of the classifiers, one can deduce what the advantages and limitations of the algorithm are. In case of advantages, the most prominent one is the accuracy of classification in both developed networks. Thanks to a wide range of training data, the networks have good generalizing abilities. It was shown that the network can work for different quality indices' type and therefore could be developed with any other type of conformity assessment. Potentially, GRU-based, deep neural networks capture patterns in provided data, so if it were trained on real-world data, the applicability is there. Despite these advantages, validating the performance of the proposed model on actual ship magnetic signatures is critical for assessing its generalization capability. When it comes to limitations, these can be listed as:

- A large (50 000 samples in the first case) dataset necessary to train the network well
- Need for data augmentation, which possibly introduces bias, that is not present in real data
- Long training time, especially when compared to statistical compliance indicators
- The increase of the number of classes corresponds to worse performance of the network, therefore the resolution of classification is restricted.
- Still based on statistical indicators (RMSE etc.)
- The optimal structure of the network needs to be experimentally found
- The lowest compliance level and width of the classes is chosen arbitrarily

Despite these disadvantages, the developed classifier may be treated as a very useful tool for models' compliance verification. Table 6 summarises analogous features to those in table 1 of the authors' solutions.

In conclusion, the use of deep learning techniques, particularly RNNs with GRU layers, showed promising results in the classification of ships' magnetic signatures and classification of ship attributes. These methods have the potential to significantly enhance naval operations, particularly in mine detection, as well as in vessel identification. Future work could involve further refinement of the models, exploring additional features, and testing them on real-world datasets for practical deployment.

Using the developed method, in addition to assessing the quality of the compatibility of the developed model with the original, one can also estimate the compatibility of the acquired object information with the available resources in the object database. The information on the size of ships and their types can be used in general for analysis for maritime transport, in economic and safety aspects and for detailed issues of analysis of traffic through straits, entrances and exits of ports.

APPENDIX
DETAILS OF THE FEM SIMULATION

The FEM environment setup of both the corvette and tugboat are described in table 7.

TABLE 7. FEM simulation details.

Parameter	Corvette	Tugboat
Relative magnetic permeability	200	200
Hull sheet thickness	0.01	0.01
No. of nodes	1307089	1196085
No. of edges	7291518	7796946
Total no. of elements	5896410	6317300
Time of calculations	11 min	22 min

REFERENCES

[1] A. Zaknich, *Neural Networks for Intelligent Signal Processing*, vol. 4. Singapore: World Scientific, 2003.
[2] S. Hochreiter and J. Schmidhuber, "Long short-term memory," *Neural Comput.*, vol. 9, no. 8, pp. 1735–1780, Nov. 1997.
[3] P. Wang, A. Jiang, X. Liu, J. Shang, and L. Zhang, "LSTM-based EEG classification in motor imagery tasks," *IEEE Trans. Neural Syst. Rehabil. Eng.*, vol. 26, no. 11, pp. 2086–2095, Nov. 2018.
[4] X. Bai, "Text classification based on LSTM and attention," in *Proc. 13th Int. Conf. Digit. Inf. Manage. (ICDIM)*, Berlin, Germany, Sep. 2018, pp. 29–32.
[5] Y. Tatsunami and M. Taki, "Sequencer: Deep LSTM for image classification," in *Proc. Adv. Neural Inf. Process. Syst.*, vol. 35, 2022, pp. 38204–38217.

[6] K. Smagulova and A. P. James, "A survey on LSTM memristive neural network architectures and applications," *Eur. Phys. J. Special Topics*, vol. 228, no. 10, pp. 2313–2324, Oct. 2019.

[7] K. Cho, B. van Merrienboer, C. Gulcehre, D. Bahdanau, F. Bougares, H. Schwenk, and Y. Bengio, "Learning phrase representations using RNN encoder–decoder for statistical machine translation," in *Proc. Conf. Empirical Methods Natural Lang. Process. (EMNLP)*, 2014, pp. 1724–1734.

[8] P. T. Yamak, L. Yujian, and P. K. Gadosey, "A comparison between ARIMA, LSTM, and GRU for time series forecasting," in *Proc. 2nd Int. Conf. Algorithms, Comput. Artif. Intell.*, 2019, pp. 49–55.

[9] R. Zhao, D. Wang, R. Yan, K. Mao, F. Shen, and J. Wang, "Machine health monitoring using local feature-based gated recurrent unit networks," *IEEE Trans. Ind. Electron.*, vol. 65, no. 2, pp. 1539–1548, Feb. 2018.

[10] R. Rana, "Gated recurrent unit (GRU) for emotion classification from noisy speech," 2016, *arXiv:1612.07778*.

[11] K. Unnikrishnan, "Artificial neural network (ANN) for modelling Earth's magnetic field belonging to solar minimum observed at a low latitude station alibag," *Indian J. Radio Space Phys.*, vol. 41, no. 3, pp. 359–366, 2012.

[12] S. T. Spantideas, A. E. Giannopoulos, N. C. Kapsalis, and C. N. Capsalis, "A deep learning method for modeling the magnetic signature of spacecraft equipment using multiple magnetic dipoles," *IEEE Magn. Lett.*, vol. 12, pp. 1–5, 2021.

[13] Y. Wang, G. Zhou, K. Wang, and X. Zhu, "Prediction on the induced magnetic signature of ships using genetic neural network," in *Proc. 16th Annual Conf. China Electrotech. Soc.*, vol. 2, 2022, pp. 592–605.

[14] F. Nurindrawati and J. Sun, "Predicting magnetization directions using convolutional neural networks," *J. Geophys. Res., Solid Earth*, vol. 125, no. 10, Oct. 2020, Art. no. e2020JB019675.

[15] Z. Hu, S. Liu, X. Hu, L. Fu, J. Qu, H. Wang, and Q. Chen, "Inversion of magnetic data using deep neural networks," *Phys. Earth Planet. Interiors*, vol. 311, Feb. 2021, Art. no. 106653.

[16] A.-I. Sasaki, "Effectiveness of artificial neural networks for solving inverse problems in magnetic field-based localization," *Sensors*, vol. 22, no. 6, p. 2240, Mar. 2022.

[17] K. Hwang, "3-D defect profile reconstruction from magnetic flux leakage signatures using wavelet basis function neural networks," Bell & Howell Inf. Learn. Co., Iowa State Univ., Ames, IA, USA, Tech. Rep. 9962823, 2000.

[18] B. Bernstein, Y. Li, and R. Hammack, "Automated metallic pipeline detection using magnetic data and convolutional neural networks," in *Proc. 2nd Int. Meeting Appl. Geosci. Energy*, Aug. 2022, pp. 1160–1164.

[19] B. Shi, X. Chen, Z. He, H. Sun, and R. Han, "Research on gesture recognition system using multiple sensors based on Earth's magnetic field and 1D convolution neural network," *Appl. Sci.*, vol. 13, no. 9, p. 5544, Apr. 2023.

[20] Y. Wang, Q. Han, G. Zhao, M. Li, D. Zhan, and Q. Li, "A deep neural network based method for magnetic anomaly detection," *IET Sci., Meas. Technol.*, vol. 16, no. 1, pp. 50–58, Jan. 2022.

[21] M. M. H. Imran, S. Jamaludin, and A. F. Mohamad Ayob, "A critical review of machine learning algorithms in maritime, offshore, and oil & gas corrosion research: A comprehensive analysis of ANN and RF models," *Ocean Eng.*, vol. 295, Mar. 2024, Art. no. 116796.

[22] A. Modi and F. Kazi, "Electromagnetic signature reduction of ferromagnetic vessels using machine learning approach," *IEEE Trans. Magn.*, vol. 55, no. 8, pp. 1–6, Aug. 2019.

[23] M. Woloszyn, J. Tarnawski, and J. Woloszyn, "Decomposition of the induced magnetism degaussing problem for fast determination of currents in demagnetization coils wrapped outside an object under arbitrary external field conditions," *J. Magn. Magn. Mater.*, vol. 580, Aug. 2023, Art. no. 170898.

[24] M. Woloszyn and J. Tarnawski, "Magnetic signature reproduction of ferromagnetic ships at arbitrary geographical position, direction and depth using a multi-dipole model," *Sci. Rep.*, vol. 13, no. 1, Sep. 2023, Art. no. 14601.

[25] M. Woloszyn and J. Tarnawski, "Minimization of a ship's magnetic signature under external field conditions using a multi-dipole model," *Sci. Rep.*, vol. 14, no. 1, Apr. 2024, Art. no. 7864.

[26] X. Jie, C. Jinfang, H. Guangjin, and Y. Xiudong, "A neural network recognition model based on ship acoustic-magnetic field," in *Proc. 4th Int. Symp. Comput. Intell. Design*, vol. 1, Hangzhou, China, Oct. 2011, pp. 135–138.

[27] C. Zuo, M. Ma, M. Li, Y. Pan, H. Yan, J. Wang, P. Geng, and J. Ouyang, "Calculation method of ship's external magnetic field based on neural network," *J. Phys., Conf. Ser.*, vol. 2363, no. 1, Nov. 2022, Art. no. 012025.

[28] K. Zielonacki and J. Tarnawski, "Neural network model of ship magnetic signature for different measurement depths," in *Proc. 28th Int. Conf. Methods Models Autom. Robot. (MMAR)*, Aug. 2024, pp. 328–333.

[29] J. A. A. Arantes Do Amaral, P. L. Botelho, N. F. F. Ebecken, and L. P. Caloba, "Ship's classification by its magnetic signature," in *Proc. IEEE Int. Joint Conf. Neural Netw.; IEEE World Congr. Comput. Intell.*, vol. 3, Apr. 1998, pp. 1889–1892.

[30] B. Kolukisa, V. C. Yildirim, B. Elmas, C. Ayyildiz, and V. C. Gungor, "Deep learning approaches for vehicle type classification with 3-D magnetic sensor," *Comput. Netw.*, vol. 217, Nov. 2022, Art. no. 109326.

[31] M. Barzegaran, A. Mazloomzada, and O. Mohammed, "Fault diagnosis of the asynchronous machines through magnetic signature analysis using finite-element method and neural networks," in *Proc. IEEE Power Energy Soc. Gen. Meeting*, Jul. 2015, p. 1.

[32] K. Kwan, S. Reford, D. M. Abdoul-Wahab, D. H. Pitcher, N. Bournas, A. Prikhodko, G. Plastow, and J. M. Legault, "Supervised neural network targeting and classification analysis of airborne EM, magnetic and gamma-ray spectrometry data for mineral exploration," *ASEG Extended Abstr.*, vol. 2015, no. 1, pp. 1–5, Dec. 2015.

[33] F. I. Hasib, N. F. Swarna, and M. A. Alam, "Classification of different magnetic structures from image data using deep neural networks," in *Proc. IEEE Asia–Pacific Conf. Comput. Sci. Data Eng. (CSDE)*, Dec. 2021, pp. 1–6.

[34] J. Tarnawski, A. Cichocki, T. A. Rutkowski, K. Buszman, and M. Woloszyn, "Improving the quality of magnetic signature reproduction by increasing flexibility of multi-dipole model structure and enriching measurement information," *IEEE Access*, vol. 8, pp. 190448–190462, 2020.

[35] M. S. Nilsson, "Modelling of civilian ships' ferromagnetic signatures," Norwegian Defence Res. Establishment, Kjeller, Norway, Tech. Rep. FFI-RAPPORT 16/00914a, 2016.

[36] J. J. Holmes, "Reduction of a ship's magnetic field signatures," in *Synthesis Lectures on Computational Electromagnetics (SLCE)*, vol. 23. San Rafael, CA, USA: Morgan & Claypool Publishers, 2008, pp. 1–76.

[37] J. Tarnawski, K. Buszman, M. Woloszyn, T. A. Rutkowski, A. Cichocki, and R. Józwiak, "Measurement campaign and mathematical model construction for the ship zodiak magnetic signature reproduction," *Measurement*, vol. 186, Dec. 2021, Art. no. 110059.

[38] J. Tarnawski, K. Buszman, M. Woloszyn, and B. Puchalski, "The influence of the geographic positioning system error on the quality of ship magnetic signature reproduction based on measurements in sea conditions," *Measurement*, vol. 229, Apr. 2024, Art. no. 114405.

[39] A. A. Kaufman and D. Alekseev, *Principles of Electromagnetic Methods in Surface Geophysics* (Methods in Geochemistry and Geophysics), vol. 45. Amsterdam, The Netherlands: Elsevier, 2014.

[40] J.-O. Hall, H. Claésson, J. Kjäll, and G. Ljungdahl, "Decomposition of ferromagnetic signature into induced and permanent components," *IEEE Trans. Magn.*, vol. 56, no. 2, pp. 1–6, Feb. 2020.

[41] (2024). *Simulia Opera Simulation Software*. Accessed: Feb. 6, 2024. [Online]. Available: https://www.3ds.com/products-services/simulia/productsopera

[42] MathWorks. (2024). *Deep Learning Toolbox*. Accessed: Feb. 6, 2024. [Online]. Available: https://www.mathworks.com/help/deeplearning

[43] L. Yang and A. Shami, "On hyperparameter optimization of machine learning algorithms: Theory and practice," *Neurocomputing*, vol. 415, pp. 295–316, Nov. 2020.

[44] D. Soekhoe, P. Van Der Putten, and A. Plaat, "On the impact of data set size in transfer learning using deep neural networks," in *Proc. 15th Int. Symp. Adv. Intell. Data Anal.*, Stockholm, Sweden. Cham, Switzerland: Springer, Oct. 2016, pp. 50–60.

[45] G. M. Foody, M. B. Mcculloch, and W. B. Yates, "The effect of training set size and composition on artificial neural network classification," *Int. J. Remote Sens.*, vol. 16, no. 9, pp. 1707–1723, Jun. 1995.

KAJETAN ZIELONACKI was born in Gdynia, Poland, in 2000. He received the B.Eng. and M.Eng. degrees in automatics and robotics from Gdańsk University of Technology, in 2023 and 2024, respectively, where he is currently the Ph.D. degree. His research interests include programmable logic controllers, optimal control, evolutionary algorithms, machine learning, and modeling magnetic signatures.

JAROSŁAW TARNAWSKI was born in Gdańsk, in 1974. He received the M.Sc. and Ph.D. degrees from Gdańsk University of Technology, in 2000 and 2006, respectively. He is a Supervisor in industrial class infrastructure, including DCS, PLC, SCADA systems, and industrial IT networks with the Computer Control Systems Laboratory. He has experience in control of drinking water supply systems and nuclear power control systems. He is currently an Assistant Professor with the Department of Electrical Engineering, Control Systems and Computer Science, Gdańsk University of Technology. His research interests include mathematical modeling, identification, optimization, hierarchical control systems, and adaptive and predictive control for objects with time-varying delays. His current research interests focus on the issue of mathematical modeling of magnetic signatures and systems for their automatic minimization. He is the co-author of ten publications in this field.

MIROSLAW WOLOSZYN was born in Gdynia, in 1963. He received the M.Sc., Ph.D., and D.Sc. (Habilitation) degrees from Gdańsk University of Technology, in 1987, 1997, and 2013, respectively. Since 1987, he has been with Gdańsk University of Technology, where he is currently an Associate Professor of electrical engineering. He is also a Principal Investigator in national project and a lead Researcher in several other national projects. He has authored or co-authored over 150 scientific and technical articles. His research interests include localization and identification of ferromagnetic objects by means of magnetometric method, magnetometric systems for object detection, ship degaussing systems, and measurement systems for ship-induced physical fields. He has been a member of Polish Society for Theoretical and Applied Electrical Engineering, since 1997.